Supporting Information

Using Liquid Crystals to Probe the Organization of Helical Polypeptide Brushes Induced by Solvent Pretreatment

Michael Tsuei[1†], Hai Tran[1†], Sangchul Roh[1], Christopher K. Ober[2]*, and Nicholas L. Abbott[1]*

[1] Smith School of Chemical and Biomolecular Engineering, Cornell University, Ithaca, NY 14853, USA

[2] Department of Materials Science and Engineering, Cornell University, Ithaca, New York 14853, USA

* Corresponding authors: christopher.ober@cornell.edu and nabbott@cornell.edu

[†] These authors contributed equally to this work.

Table of Contents:

Section S1. PBLG Molecular Weight and Grafting Density Calculation

For 50 nm-thick quenched PBLG brushes, the average PBLG chain tilt angle with respect to the surface normal is 20.2 ± 0.8°. We calculated the PBLG molecular weight from these measurements using the method reported by Lee and Frank[1], as shown below:

In the calculations below, we assume that the PBLG chains are straight and not bent, since the average axial length of the PBLG chains is similar to the persistence of length of PBLG[2] (87.5 ± 10 nm).

The length of the PBLG chain (l) is calculated as

$$l = \frac{50\ \text{nm}}{\sin(90° - 20.2°)} = 53.2\ \text{nm} \quad (1)$$

As each monomer unit of PBLG contributes 1.5 Å to the length of the helical axis of the chain, the degree of polymerization is calculated as

$$DP = \frac{53.2\ \text{nm}}{0.15\ \text{nm}} = 353 \quad (2)$$

The molecular weight of the polymer is therefore calculated as

$$MW = 353\ \times 219\ \text{g/mol} = 77307\ \text{g/mol} \quad (3)$$

where the molecular weight of the PBLG monomer unit is 219 g/mol

We checked the validity of the methodology described above using additional experimental data found in the published literature[3]. Specifically, Wang and Chang[3] report PBLG brush thickness measurements and PBLG chain tilt angles (obtained from FT-IR spectroscopy) for PBLG brushes before quenching (thickness: 94.6 nm, PBLG tilt: 49° from the surface normal) and after quenching (thickness: 165.9 nm peak-to-valley teepee height, PBLG tilt: 3° from the surface normal). Below, we calculate the molecular weight of the same PBLG brush in the two different above-mentioned organizations and assess whether a consistent molecular weight for PBLG is obtained by the methodology.

Molecular weight estimation of PBLG brushes before quenching

PBLG brush thickness = 94.6 nm

Axial length of the PBLG chain= 946 Å/sin(90 - 49°) = 1,442 Å

Monomer unit length = 1.5 Å

Degree of polymerization (DP) = 1442 Å/1.5 Å = 961

γ-benzyl-L-glutamate unit molecular weight (MW) = 219 g/mol

PBLG molecular weight (MW) = 961 x 219 g/mol **= 210,459 g/mol**

Molecular weight estimation of PBLG brushes after quenching

PBLG brush thickness = 165.9 nm

Axial length of the PBLG chain = 1659 Å/sin(90-3°) = 1,661 Å

Monomer unit length = 1.5 Å

Degree of polymerization (DP) = 1,661 Å/1.5 Å = 1,107

γ-benzyl-L-glutamate unit molecular weight (MW) = 219 g/mol

Quenched PBLG molecular weight (MW) = 1,107 x 219 g/mol **= 242,433 g/mol**

The calculations above show that molecular weights estimated for the PBLG brush before and after quenching are similar. This provides additional support for the methodology that we have used to estimate the molecular weight of the PBLG used in our study.

We use this estimated molecular weight to calculate the grafting density of the PBLG brush

The grafting density (σ) is calculated as

$$\sigma = \frac{h_{col}\rho N_A}{M_n} = \frac{38.7\text{nm x}\frac{1.32\text{g}}{\text{cm}^3}\text{x } 10^{-21}\frac{\text{cm}^3}{\text{nm}^3}\text{x } 6.02{*}10^{23}\text{chains/mol}}{77307\text{g/mol}} = 0.397\ \text{chain/nm}^2 \quad (4)$$

, where h_{col}, ρ, and N_A are the PBLG brush thickness before quenching, polymer density and the Avogadro number respectively.

Polymer brush thickness before quenching (average PBLG chain tilt before quenching = 43 ± 0.3°) is

$$h_{col} = l \times \sin(90° - 43°) = 38.7\ \text{nm} \quad (5)$$

Section S2. Estimation of Average PBLG Tilt Angle via FTIR

We estimated the average tilt angles of the PBLG in the collapsed and quenched brushes using the dichroic ratio from two characteristic amide peaks (amide I - 1654 cm^{-1} and amide II - 1550 cm^{-1}) via FTIR. Using Equation 6 below,[4] we estimated the average tilt angles with respect to the surface normal of the collapsed and quenched PBLG brushes to be 43.0 ± 0.3° and 20.2 ± 0.8°, respectively

$$R = A_{Amide\ I}/A_{Amide\ II} = K\frac{[\sin^2\theta\cos^2\alpha_I + \frac{1}{2}\sin^2\alpha_I(1+\cos^2\theta)]}{[\sin^2\theta\cos^2\alpha_{II} + \frac{1}{2}\sin^2\alpha_{II}(1+\cos^2\theta)]} \quad (6)$$

where, R is the dichroic ratio of the amide I and amide II bands, $A_{Amide\ I}$ is the area under the amide I band, $A_{Amide\ II}$ is the area under the amide II band, K (3.6) is a proportionality constant calculated from the transmission FTIR spectrum of a polyglutamate Langmuir Blodgett film, α_I and α_{II} are transition dipole moment angles of the amide I (39° from helical axis) and amide II (75° from helical axis) bands respectively,[5] and θ is the average PBLG helix tilt angle.

Section S3. LC Tilt Estimation

We estimated the LC tilt angle at the PBLG brush interface assuming that the orientation of the LC within the film is dominated by the elastic free energy of the LC. For LC systems in which the LC at the air-LC interface adopts homeotropic orientation (θ_{air} = 0°), the relationship between the optical retardance of the LC film with thickness (d) and the LC tilt angle at the bottom PBLG interface ($\theta_{surface}$ measured from the surface normal) is described by equation 7,[6] below:

$$\Delta r \approx \int_0^d \left(\frac{n_0 n_e}{\sqrt{n_0^2\sin^2\left(\theta_{surface}*\frac{z}{d}\right)+n_e^2\cos^2\left(\theta_{surface}*\frac{z}{d}\right)}} - n_0\right) dz \quad (7)$$

where n_0 (1.53) and n_e (1.71) are the indices of refraction perpendicular (ordinary axis) and parallel (extraordinary axis) to the optical axis of 5CB, respectively.
The retardance of LC films comprising LC-filled metal TEM grids that were supported on an untreated glass substrate in air (homeotropic at LC-air interface & $\theta_{surface}$ = 90°) was estimated to be Δr = 1900 nm via comparison of the optical appearance of the LC film with the Michel-Levy color chart. We used this estimated retardance of the LC film in equation 7 to solve for the thickness of the LC film (19.7 μm). We assume that the LC film thickness is constant among samples. We then supported LC films on PBLG brushes and we used equation 7 to estimate the characteristic LC tilt angle ($\theta_{surface}$) at the PBLG brush surface. The retardance of the LC was estimated from the color observed via optical microscopy (Figure 2b) using the Michel-Levy chart. For 50 nm-thick PBLG brushes, we estimated the retardance (Δr) to be 1833 ± 58 nm.

We validated use of the Michel-Levy chart to estimate the LC tilt angle by performing independent measurements of the optical birefringence using a Berek compensator. By using optical interference colors in Figure 2d, a Michel-Levy chart and equation 7, we determined that the LC tilt angle at the brush interface of the sample shown in Figure 2d is 87 ± 2° from the surface normal. This estimated LC tilt angle is consistent with direct measurements of LC tilt angle using a Berek Compensator, which yields a LC tilt angle at the brush interface of 89 ± 1° from the surface normal.

Section S4. Effect of PBLG Brush Pretreatment with 5CB on PBLG Tilt Angle

Table S1: Average PBLG tilt angles of brushes treated with either chloroform or acetone before and after 15 min incubation of brushes in 5CB.

50 nm PBLG	Collapsed (Tilt Angle)	Quenched (Tilt Angle)
NO LC	43 ± 1°	20 ± 1°
LC Treated	43 ± 1°	19 ± 1°

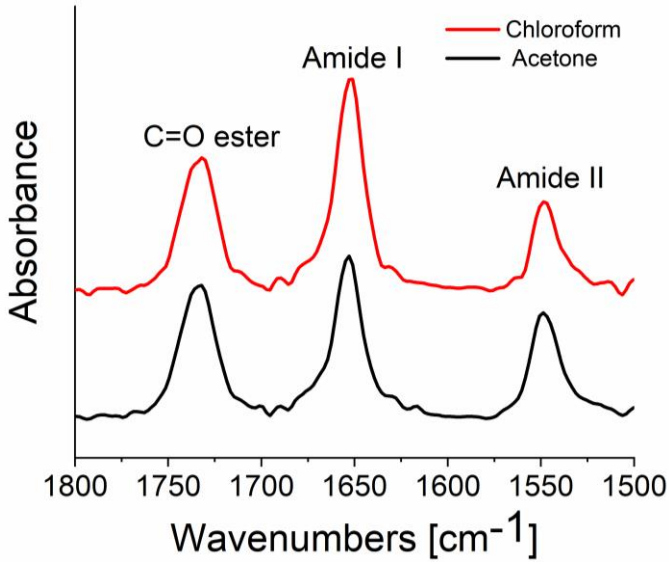

Figure S1: FTIR spectra of 50 nm-thick PBLG brushes treated with chloroform (red) and acetone (black), and subsequently incubated in LC prior to rinsing off the LC with acetone (poor solvent) and drying. The labeled peaks are amide I (1654 cm^{-1}, backbone carbonyl stretching) and amide II (1550 cm^{-1}, C-N stretching) of the α-helices, and the ester side chain (1734 cm^{-1}).[7]

Average PBLG tilt angles were obtained via FTIR measurements of both chloroform and acetone treated 50 nm-thick PBLG brushes. The brushes were then incubated in thick films of 5CB for 15 minutes and subsequently rinsed off with acetone. The average PBLG tilt angles of the LC-treated brushes were measured using FTIR, which showed no significant change in the average tilt angle of PBLG chains. This result suggests that 5CB is a poor solvent for PBLG, and thus does not influence the organization of PBLG chains.

Section S5. LC Response to Initiator-functionalized Substrates and PBLG Thin Films

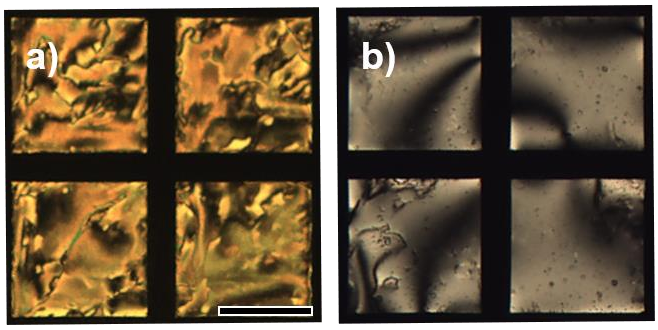

Figure S2: Optical micrographs between crossed polarizers of 20 μm-thick LC films supported on a) 3-aminopropyldimethylethoxysilane (APDMES; initiator)-functionalized substrate, and b) PBLG thin film in the absence of initiator. Scale bar is 200 μm.

We performed two controls to determine the LC response to both the initiator that tethers PBLG chains to the solid substrate and free PBLG in the absence of initiator. In our first control system, a glass substrate was functionalized with initiator (3-aminopropyldimethylethoxysilane (APDMES)) and subsequently contacted with a 20 μm-thick LC film. The LC films in contact with initiator-functionalized substrates exhibited a bright optical texture, when viewed between crossed polarizers, indicative of tilted/planar alignment of LCs (see Figure S2a). In our second control, we observed that LCs in contact with a thin film of PBLG free of initiator, that was formed by depositing chloroform-solubilized PBLG chains from solution onto a glass substrate via evaporation, exhibited planar alignment (see Figure S2b). The controls described above indicate that differences in LC response between collapsed and quenched PBLG brushes is a consequence of a change in the organization of the brush.

Section S6. PBLG Brushes Change the Easy Axis of LCs

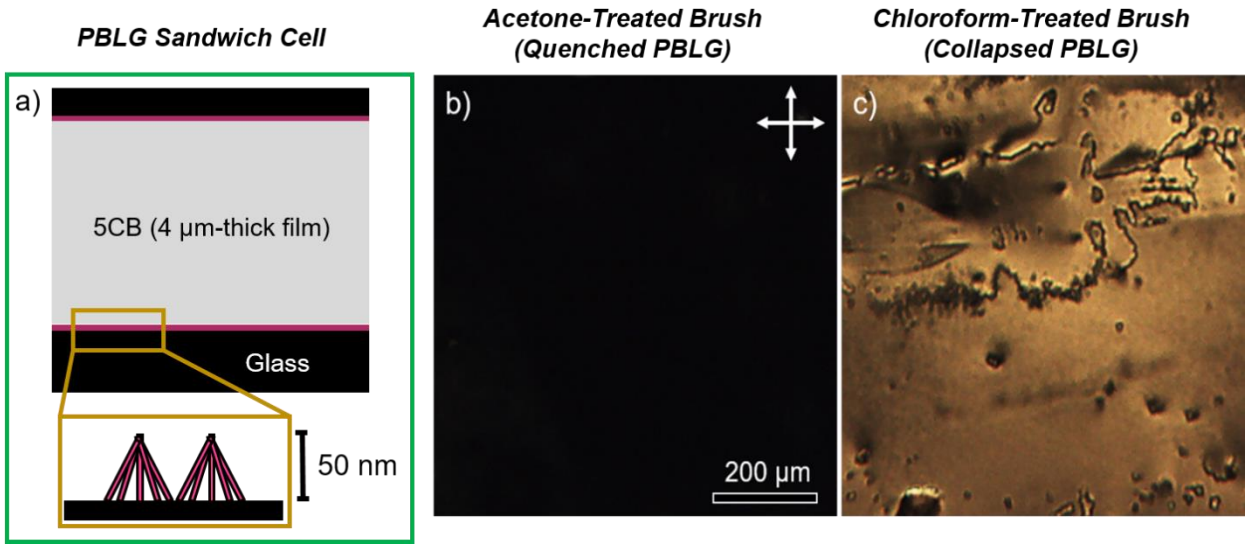

Figure S3: a) Schematic illustration of 4 μm-thick LC film confined between two 50 nm-thick PBLG brushes treated with either b) acetone or c) chloroform. When viewed between crossed polarizers, b) homeotropic alignment of LCs was observed for the LC films confined between acetone-quenched brushes, and c) planar alignment of LCs was observed for LC films confined between chloroform-collapsed brushes.

As described in the main text, 20 μm-thick LC films with boundary conditions of air and PBLG brushes that were pretreated with either chloroform or acetone exhibited different optical textures. We determined if the observed difference in LC alignment for chloroform and acetone-treated brushes was a result of a decrease in the surface anchoring energy of the LC or a change in the easy axis of the LCs by confining LC films between 2 glass slides decorated with 50 nm-thick PBLG brushes that were pretreated with either chloroform or acetone and separated by 4 μm diameter glass spacers. For LC films confined between acetone-treated brushes, a dark optical texture was observed when viewed between crossed polarizers, indicating homeotropic alignment of the LC. In contrast, LC films confined between chloroform treated-brushes exhibited a bright optical texture indicating non-homeotropic alignment of the LC. This result indicates that PBLG brushes change the easy axis of the LC.

Section S7. 2D and 3D Height Profiles of PBLG Brushes via AFM

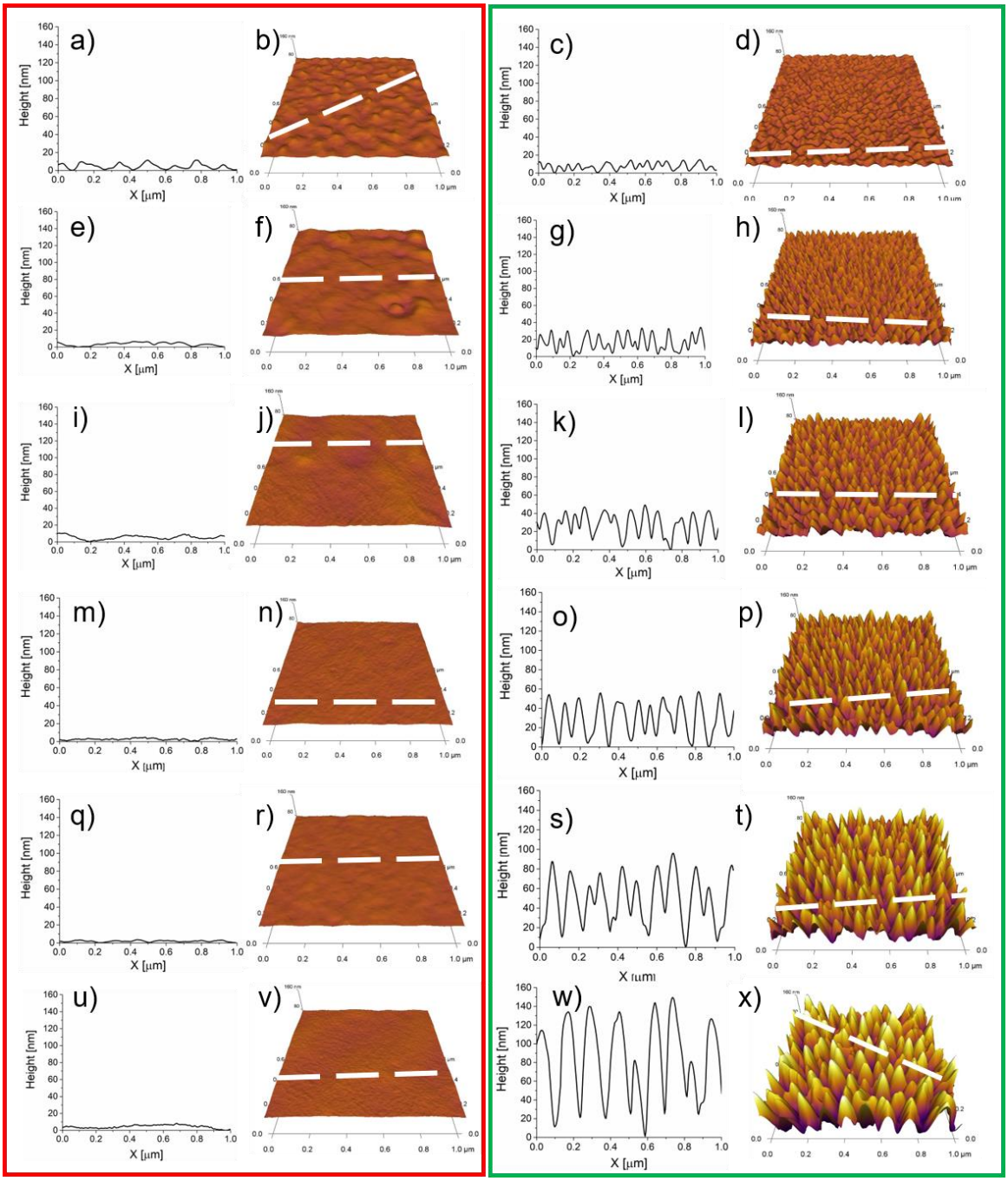

Figure S4: 2D and 3D height profiles obtained via AFM for chloroform-collapsed (red box) and acetone-quenched (green box) PBLG brushes with thicknesses of a-d) 12 nm, e-h) 25 nm, i-l) 40 nm, m-p) 50 nm, q-t) 80 nm, u-x) 140 nm

We performed AFM measurements on PBLG brushes with a range of brush thicknesses (12, 25, 40, 50, 80, 140 nm). These measurements revealed that the tilt angles of brushes treated with chloroform diverge from those of brushes treated with acetone with increasing brush thickness.

Section S8. LC Response to PBLG Brushes of Variable Thickness

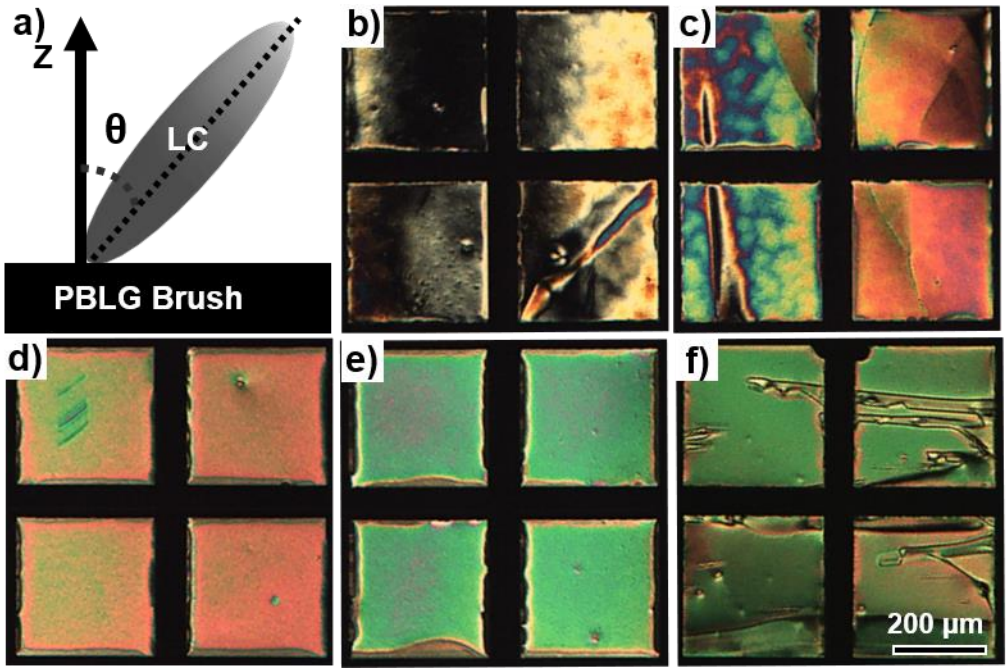

Figure S5: (a) Schematic illustration of LC tilt at PBLG brush interface and (b-e) micrographs (crossed polarizers) of LC thin films on chloroform-treated PBLG brush with (b,c) thickness (z) gradient of (b) z= 16-20 nm (increasing left to right), (c) z= 25-32 nm (increasing left to right), (d) z= 32 nm, (e) z= 40 nm, (f) z= 50 nm.

We found that 20 μm-thick LC films supported on chloroform-treated PBLG brushes of different thicknesses exhibited different optical textures indicating different LC tilt angles that result from different averaged PBLG tilt angles. Tilt angles of the LCs were calculated using equation 7 in Section S3. These calculated tilt angles (Figure 4f) showed that LC tilt from the surface normal increased with increasing PBLG brush thickness.

Section S9. Probing Intermolecular Interactions Between LCs and PBLG

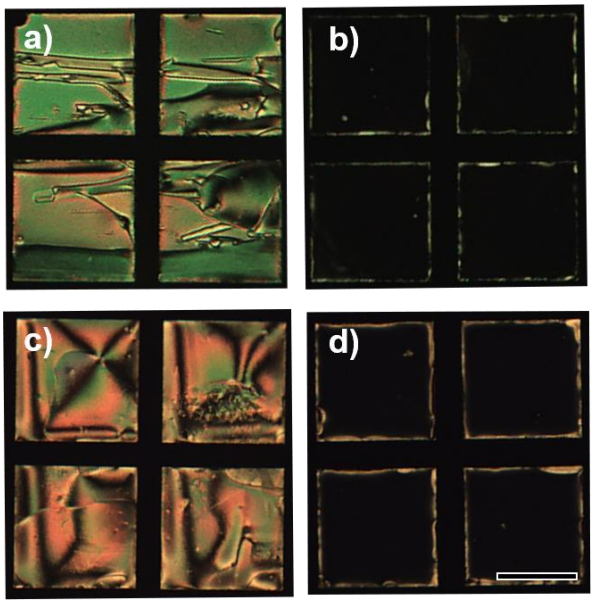

Figure S6: Optical micrographs of 20 μm-thick a,b) 5CB and c,d) MBBA film supported on a,c) chloroform-collapsed and b,d) acetone-quenched 50 nm-thick PBLG brushes between crossed polarizers. Scale bar is 200 μm.

Our FTIR and LC results suggest that intermolecular interactions between PBLG and LCs control LC orientation Past studies have demonstrated that van der Waals interactions are central in dictating LC ordering near solid interfaces such as rubbed polymer films[8,9] and self-assembled alkanethiol monolayers[10,11]. In these studies, the optical axes of the LC and PBLG align to generate the strongest van der Waals coupling. We explored the potential role of dipole interactions in inducing different LC ordering in the presence of collapsed and quenched polymer brushes by using N-(4-methoxybenzylidene)-4-butylaniline (MBBA) as the LC. In contrast to 5CB, which possesses positive dielectric anisotropy and anisotropic polarizability ($\Delta\varepsilon = +13$, $\Delta n = +0.18$),[12] MBBA possesses negative dielectric anisotropy and positive anisotropic polarizability ($\Delta\varepsilon = -0.7$, $\Delta n = +0.21$).[12] By comparison of the optical responses of 5CB (Figure S6a,b) and MBBA (Figure S6c,d), we can ascertain whether dipole or dispersion interactions are the primary driving force for LC reorientation. Specifically, if the ordering of MBBA in contact with collapsed and quenched PBLG brushes differs from that of 5CB, then dipole interactions are dominant. However, if the optical response of MBBA is similar to that of 5CB, then dispersion interactions are dominant. Subsequent to observing MBBA thin films supported on both collapsed (Figure S6c) and quenched (Figure S6d) brushes between crossed polarizers, we observed a similar response to that with 5CB. This observation led us to conclude that in our system, dispersion interactions between PBLG and LC were the primary interactions that dictated the LC response to PBLG brushes.

Section S10. Relationship Between LC and PBLG Tilt Angles

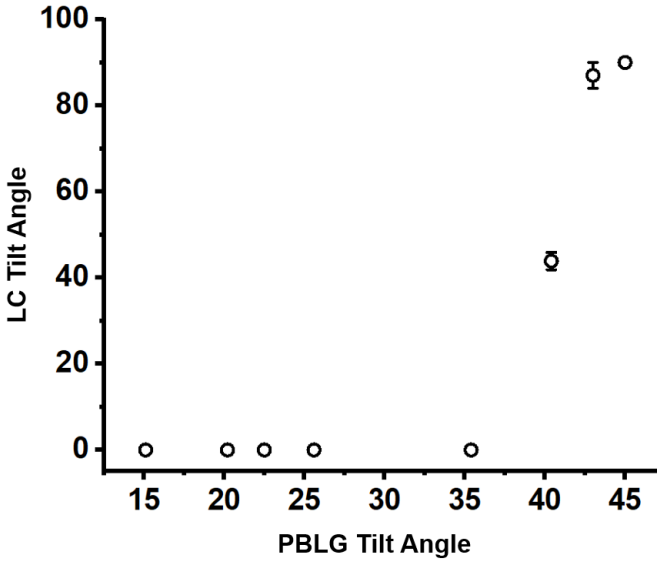

Figure S7: Average LC tilt angles from the surface normal as a function of PBLG chain tilt angle for solvent-treated PBLG brushes. Data points show mean values and the error bars represent 1 standard deviation (n=3).

The relationship between LC and PBLG tilt angles was established through direct comparison of measured PBLG (Figure 4e) and LC (Figure 4f) tilt angles for brushes of specified thickness.

Section S11. Deconvoluted FTIR Spectra of Heat-Treated 130 nm-thick PBLG Brushes

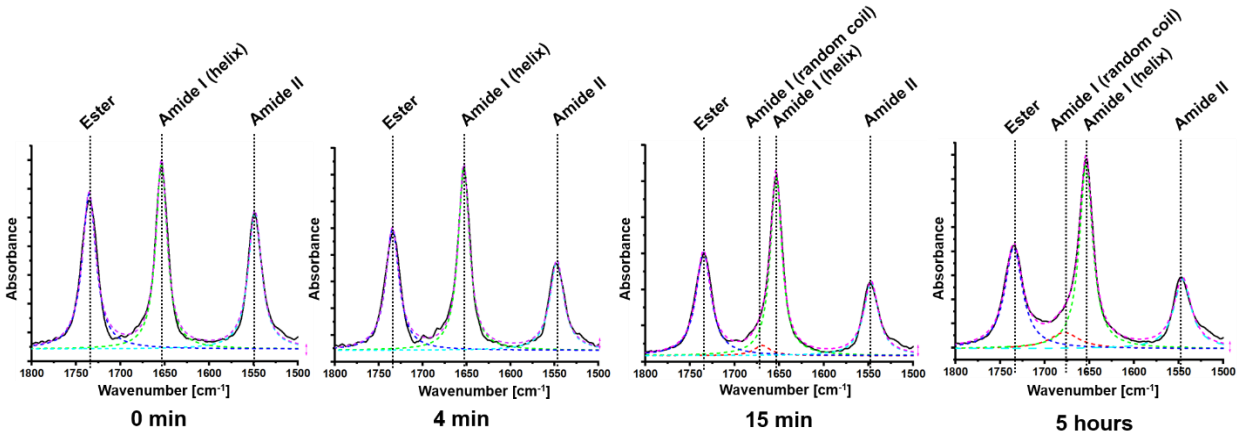

Figure S8: Deconvoluted FTIR spectra displaying the region 1800–1500 cm^{-1}, showing an increase in amide I (random coil) peak (1680 cm^{-1}) with increasing heating time of the PBLG brushes.

Section S12. FTIR Spectra of Mixed Solvent Treated 140 nm-thick PBLG Brushes

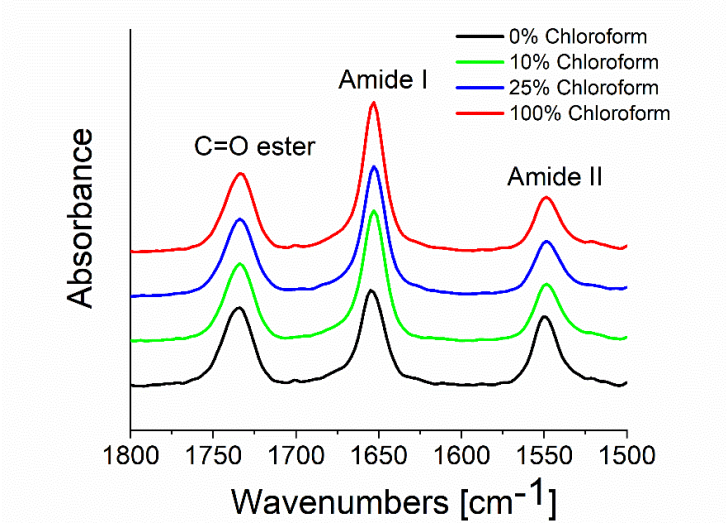

Figure S9: FTIR spectra of 140 nm thick PBLG polymer brushes treated with chloroform and acetone mixtures. Four different solvent compositions (0%, 10%, 25% and 100% chloroform in acetone) were used. The labeled peaks are amide I (1654 cm^{-1}, backbone carbonyl stretching), amide II (1550 cm^{-1}, C-N stretching) of α-helical secondary structure, and the ester side chain (1734 cm^{-1}).[7]

Section S13. Fractional Area Coverage of Homeotropic Domains in LC Film Supported on 140 nm-thick PBLG Brush Treated with Mixed Solvents

Table S2 Fractional Area Coverage for Large Circular Homeotropic Domains for 140 nm-thick PBLG brushes Treated with 10% Chloroform in Acetone.

Grid	Homeotropic Domain Areal Coverage
1	7%
2	8%
3	5%
4	6%
Average	7%
Stdev	1%

From the relationship between the LC and PBLG tilt established in Figure 4 and Section S10, we estimate an average PBLG tilt angle in each of the observed domains to be as follows. The inner domain has PBLG chain tilt of 41°, the region outside the domains has a tilt of 40°, and the large circular homeotropic domain has a chain tilt between 15° and 35° from the surface normal. Using these PBLG chain tilt angles that were estimated from the LC optical response, we calculated an averaged PBLG chain tilt across the

entire PBLG brush by weighting the contributions of the domains using their fractional area coverage. As shown in Table S2 above, the large circular homeotropic domains occupy 7 ± 1% of the film area. Since the tilt angles inside and outside of the small circular tilted LC domains are similar, we make an approximation of 40° tilt from the surface normal, which occupies the remainder of the film area (93%). Thus, we estimate the average PBLG tilt across the LC film as follows:

Assuming the large circular homeotropic domain has a chain tilt of 15° from the surface normal:

$$(15° \; x \; 0.07) + (40° \; x \; 0.93) = 38° \text{ from the surface normal}$$

Similarly, if we assuming the large circular homeotropic domain has a chain tilt of 35°:

$$(35° \; x \; 0.07) + (40° \; x \; 0.93) = 40° \text{ from the surface normal}$$

As shown above, the average PBLG tilt angle estimated via LC tilt ranges between $38° \leq \theta \leq 40°$, which is in reasonable agreement with the average PBLG tilt angle measured via FTIR (37 ± 1°).

Section S14. 2D and 3D Height Profiles of 140 nm-thick PBLG Brushes via AFM

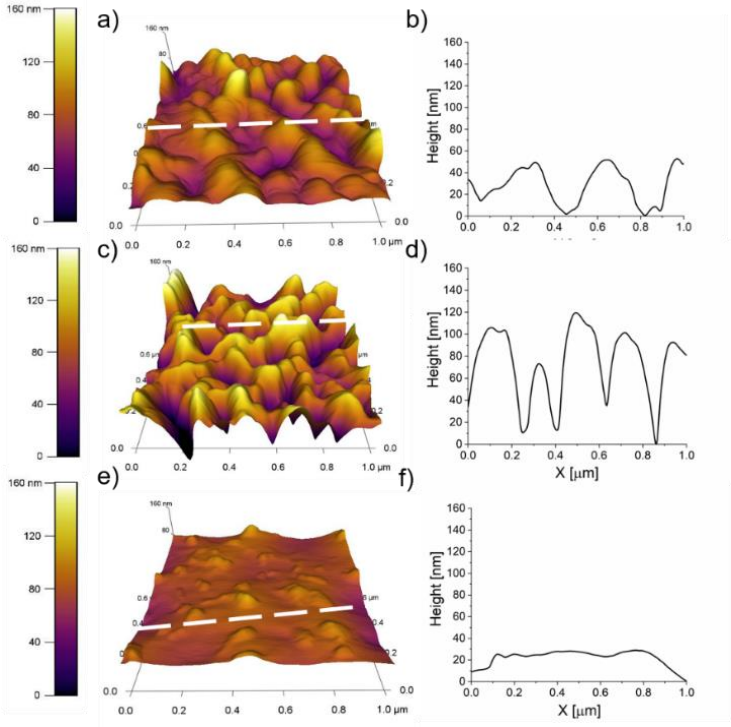

Figure S10: (a,c,d) 3D and (b,d,f) 2D height profiles measured via AFM of a,b) inner domain, c,d) ring-like region, e,f) outer continuous domain of 140 nm-thick PBLG brushes treated with 10% chloroform in acetone. Dotted white lines show cross-section of 3D profile used to generate 2D height profiles.

Section S15. 2D and 3D Height Profiles of 50 nm-thick PBLG Brushes via AFM

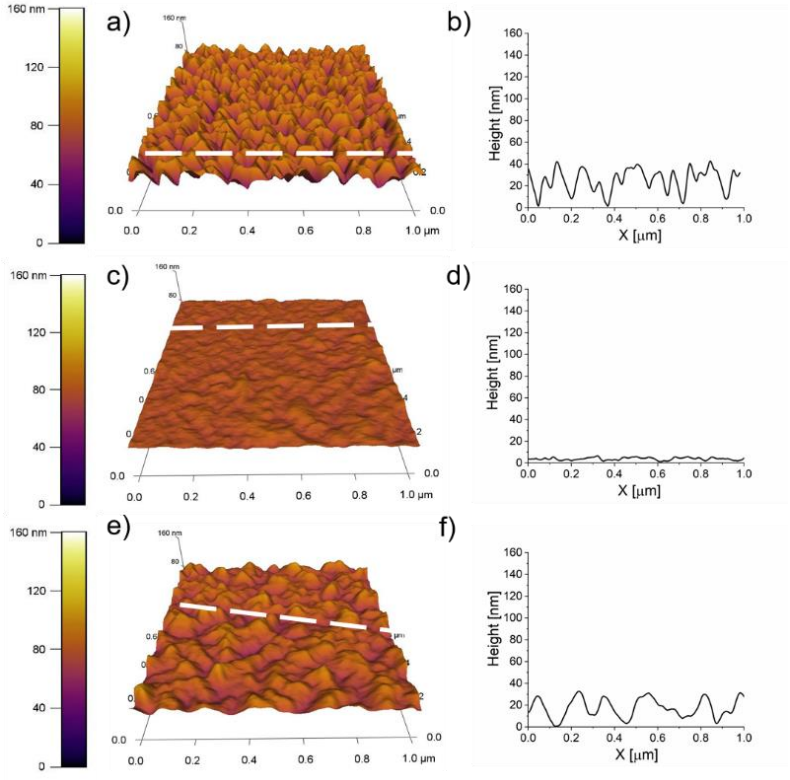

Figure S11: (a,c,e) 3D and (b,d,f) 2D height profiles measured via AFM of a,b) inner domain, c,d) ring-like region, e,f) outer continuous domain of 50 nm-thick PBLG brushes treated with 10% chloroform in acetone. Dotted white lines show cross-section of 3D profile to generate 2D height profiles.

Section S16. PBLG Brush Patterning via Nucleation of Chloroform at PBLG Brush Interfaces

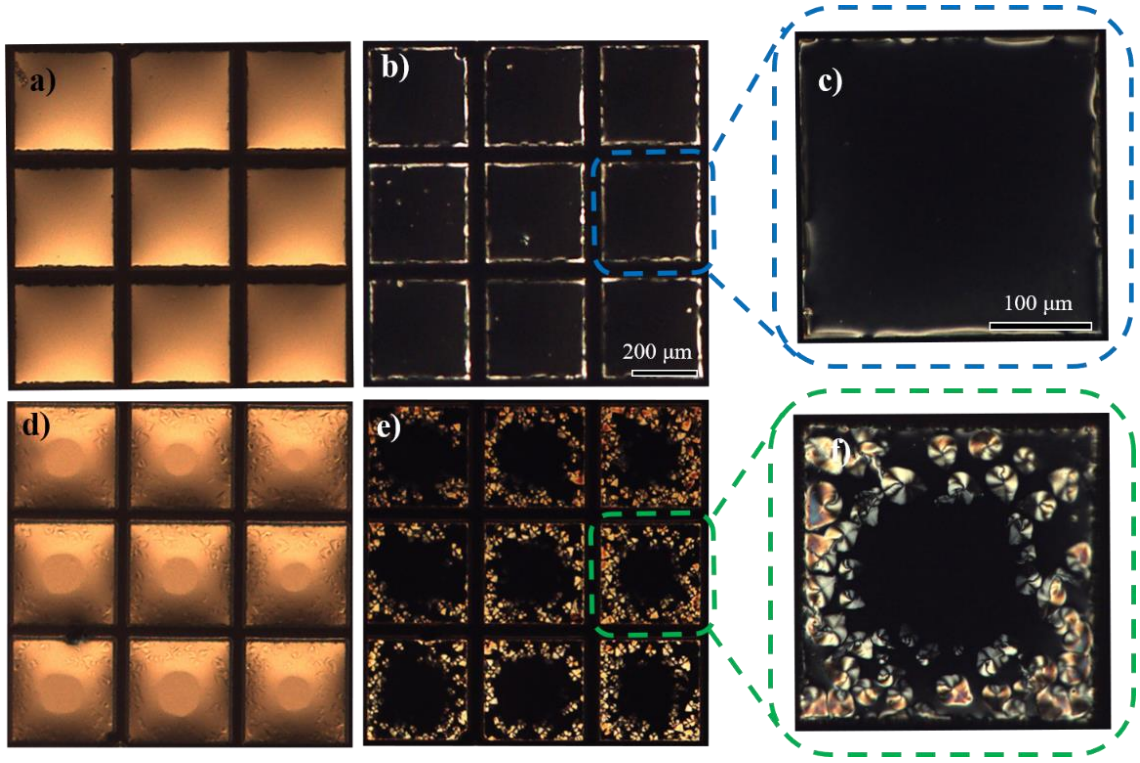

Figure S12: Micrographs of 20 µm-thick 5CB films, a,d) under bright field microscopy and b,c,e,f) between crossed polarizers, supported on acetone-quenched 140 nm-thick PBLG brushes in air after 2 hour incubation in a-c) water and d-f) water saturated with chloroform ($C_{chloroform} \leq 1\%$ v/v).

Three 140 nm-thick PBLG brushes were quenched in acetone prior to contact with LC. Following contact between the LC (5CB) and solvent quenched substrate, the LC films displayed a dark optical texture indicative of homeotropic anchoring. The LC films on solvent-quenched nanofiber substrate were then each independently incubated in 2 mL of water saturated with chloroform ($C_{chloroform\ saturate} \sim 1\%$ v/v). The saturated chloroform in water solution was prepared by mixing 1 mL chloroform with 19 mL water and equilibrating at room temperature (T=25 °C) for 3 hours. The water phase that was enriched with chloroform was collected and LC films supported on 140 nm-thick PBLG brush substrates were immersed in the chloroform-saturated water. While the LC films were within the chloroform-saturated water, the LC films transitioned to an isotropic phase, which indicated that chloroform spontaneously partitioned from the water into the LC. After incubating the LC film supported on the PBLG brush in chloroform-saturated water for 2 hours, the LC film on PBLG brushes were removed from the chloroform-saturated water and heated to 60 °C for 30 min to remove chloroform from the LC. The samples were subsequently cooled to room temperature (T=25 °C) and viewed between crossed polarizers in air, revealing micrometer-scale circular tilted LC domains similar in shape to those observed for LC films supported on 50 nm-thick PBLG brushes pretreated with chloroform-acetone mixtures. We note here, that incubation of LC films on PBLG brushes in water alone for 2 hours did not result in any change in the LC optical texture (homeotropic alignment).

References

1. Lee, N. H.; Frank, C. W., Surface-Initiated Vapor Polymerization of Various α-Amino Acids. *Langmuir* **2003**, 19, 1295-1303

2. Moha, P.; Weill, G.; Bernolt, H., Longueur de persistence du poly L glutamate de benzyle en solution. *J. Chim. Phys.* **1964**, 61, 1240-1244

3. Wang, Y.; Chang, Y. C., Preparation of Unidirectional End-grafted Alpha-helical Polypeptides by Solvent Quenching. *J. Am. Chem. Soc.* **2003**, 125 (21), 6376-6377.

4. Luijten, J.; Groeneveld, D. Y.; Nijboer, G. W.; Vorenkamp, E. J.; Schouten, A. J., Cross-linking-induced Permanently Perpendicular Helix Orientation in Surface-grafted Polyglutamate Films. *Langmuir* **2007**, 23 (15), 8163-8169.

5. Wieringa, R. H.; Siesling, E. A.; Werkman, P. J.; Angerman, H. J.; Vorenkamp, E. J.; Schouten, A. J., Surface Grafting of Poly(L-glutamates). 2. Helix Orientation. *Langmuir* **2001**, 17, 6485-6490.

6. Miller, D. S.; Carlton, R. J.; Mushenheim, P. C.; Abbott, N. L., Instructional Review: An Introduction to Optical Methods for Characterizing Liquid Crystals at Interfaces. *Langmuir* **2013**, 29 (10), 3154-3169.

7. Tran, H.; Zhang, Y.; Ober, C. K., Synthesis, Processing, and Characterization of Helical Polypeptide Rod-Coil Mixed Brushes. *ACS Macro Lett.* **2018**, 7 (10), 1186-1191.

8. Ban, B. S.; Kim, Y. B., Materials and Rubbing Dependence on Azimuthal Anchoring Energy of Rubbed Polyimide Surfaces. *J. Phys. Chem. B* **1999**, 103, 3869-3871.

9. Abbott, N. L., Surface Effects on Orientation of Liquid Crystals. *Curr. Opin. Colloid Interface Sci.* **1997**, 2, 76-82.

10. Drawhorn, R. A.; Abbott, N. L., Anchoring of Nematic Liquid Crystals on Self-Assembled Monolayers Formed from Alkanethiols on Semitransparent Films of Gold. *J. Phys. Chem.* **1995**, 99, 16511-16515.

11. Evans, S. D.; Allinson, H.; Boden, N.; Flynn, T. M.; Henderson, J. R., Surface Plasmon Resonance Imaging of Liquid Crystal Anchoring on Patterned Self-Assembled Monolayers. *J. Phys. Chem. B* **1997**, 101, 2143-2148.

12. Mushenheim, P. C.; Abbott, N. L., Hierarchical Organization in Liquid Crystal-in-Liquid Crystal Emulsions. *Soft Matter* **2014**, 10 (43), 8627-8634.